CO and H_I observations of an enigmatic interstellar cloud

Y. Libert¹, E. Gérard², T. Le Bertre¹, L.D. Matthews³, C. Thum⁴, and J.M. Winters⁴

- ¹ LERMA, UMR 8112, Observatoire de Paris, 61 Av. de l'Observatoire, 75014 Paris, France
- ² GEPI, UMR 8111, Observatoire de Paris, 5 Place J. Janssen, 92195 Meudon Cedex, France
- ³ MIT Haystack Observatory, Off Route 40, Westford, MA 01886, USA
- ⁴ IRAM, 300 rue de la Piscine, 38406 St. Martin d'Hères, France

Received March 6, 2009; accepted April 6, 2009

ABSTRACT

Context. An isolated H I cloud with peculiar properties has recently been discovered by Dedes, Dedes, & Kalberla (2008, A&A, 491, L45) with the 300-m Arecibo telescope, and subsequently imaged with the VLA. It has an angular size of $\sim 6'$, and the H I emission has a narrow line profile of width $\sim 3 \, \mathrm{km \, s^{-1}}$.

Aims. We explore the possibility that this cloud could be associated with a circumstellar envelope ejected by an evolved star.

Methods. Observations were made in the rotational lines of CO with the IRAM-30m telescope, on three positions in the cloud, and a total-power mapping in the H_I line was obtained with the Nançay Radio Telescope.

Results. CO was not detected and seems too underabundant in this cloud to be a classical late-type star circumstellar envelope. On the other hand, the H I emission is compatible with the detached-shell model that we developed for representing the external environments of AGB stars.

Conclusions. We propose that this cloud could be a fossil circumstellar shell left over from a system that is now in a post-planetary-nebula phase. Nevertheless, we cannot rule out that it is a Galactic cloud or a member of the Local Group, although the narrow line profile would be atypical in both cases.

Key words. Stars: AGB and post-AGB – (Stars:) circumstellar matter – ISM: clouds – (ISM:) planetary nebulae – Radio lines: ISM

1. Introduction

In the course of a sky survey for H_I halo clouds with the Arecibo 300-m Radio Telescope, Dedes et al. (2008, DDK2008) detected a cloud with unusual properties. It is isolated, nearly circular with an angular size of 6.4'. The H_I emission is centered at V_{lsr} = 47.6 km s⁻¹ and shows a surprisingly small linewidth of 3.4 km s^{-1} . It has a peak hydrogen column density, $N_H = 60$ 10¹⁸ cm⁻². Follow-up observations with the Very Large Array (VLA) in the D-configuration show a slightly elongated structure, oriented at PA $\sim -14^{\circ}$, and resolved into an elliptical ring of H_I emission peaks (from 1 to 1.8 10^{20} cm⁻²), of about $4' \times 3'$, with the major axis along the same direction (cf. their figure 1b). A velocity gradient of $\sim 1 \text{ km s}^{-1}$ is also seen along the major axis (their figure 1c). A faint star (2MASS 07495348+0430238) was found coincident with the density minimum at the center of the ring. The difference between the images obtained at Arecibo and with the VLA is probably an effect of the interferometric mode of observation which tends to filter extended emission (de Pater et al. 1991).

Several hypotheses are considered by DDK2008. Among them, that this enigmatic cloud, hereafter refered to as DDK cloud, is a circumstellar envelope around an evolved star. Indeed, the narrow line profile is typical of what is observed in H I around this type of source (Gérard & Le Bertre 2006, Matthews & Reid 2007). In addition the image obtained at the VLA is reminiscent of the fragmented ring, reported also in H I by Rodríguez et al. (2002), in the Planetary Nebula NGC 7293 (Helix Nebula). With this line of thought, we have obtained new data in the CO rotational lines with the IRAM 30-m telescope, and in the H I emission line at 21 cm with the Nançay Radio Telescope. In this paper, we present our results and discuss in more detail the possi-

bility that the DDK cloud is associated with the mass loss of an evolved star.

2. Observations

2.1. HI observations

New H_I data have been obtained with the Nançay Radio Telescope (NRT). This meridian telescope has a clear rectangular aperture with effective dimensions $160 \,\mathrm{m} \times 30 \,\mathrm{m}$. Thus the beam has a FWHM (full-width at half-maximum) of 4' in right ascension (RA) and 22' in declination (Dec) at 21 cm. The spatial resolution in RA is comparable to that of Arecibo. The point source efficiency is $1.4 \,\mathrm{K} \,\mathrm{Jy}^{-1}$, and the beam efficiency, 0.65.

A frequency-switch spectrum at a resolution of 0.16 km s⁻¹ was first obtained on the source, defined by the 2MASS star. Galactic H $_{\rm I}$ emission is detected from –40 to 80 km s⁻¹ with a maximum of 7.3 K at $V_{\rm lsr}=9\,{\rm km\,s^{-1}}$ (Fig. 1). The DDK cloud emission is clearly detected at $V_{\rm lsr}=+47.6\,{\rm km\,s^{-1}}$ over Galactic emission at a level of 0.6 K. The integrated Galactic emission in the DDK cloud line-of-sight is $\sim 265\,{\rm K\,km\,s^{-1}}$ which translates to a hydrogen column density, $N_{\rm H}=4.8\,10^{20}\,{\rm cm^{-2}}$. Using the standard relation, $N_{\rm H}/A_{\rm v}=1.87\,10^{21}\,{\rm cm^{-2}\,mag^{-1}}$, we derive a Galactic extinction over the line of sight, $A_{\rm v}=0.26$. This estimate brings an upper limit to the extinction towards the DDK cloud, if it is located within our Galaxy.

An additional grid of positions was mapped using the NRT. The observations have been obtained in the position-switch mode at a spectral resolution of 0.32 km s^{-1} , with again the onposition on the 2MASS star, and the off-positions at $\pm 2'$, $\pm 4'$, $\pm 6'$, $\pm 8'$, and $\pm 12'$ in the east-west direction. The analysis has been performed as for the study of EP Aqr and Y CVn (Le Bertre

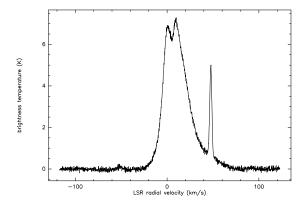


Fig. 1. Frequency-switch spectrum obtained with the NRT.

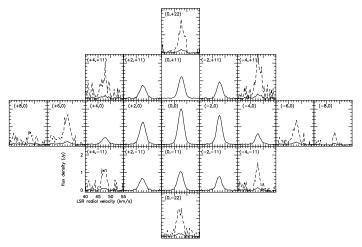


Fig. 2. Map of the 21 cm H_I emission of the DDK cloud obtained with the NRT. The central position corresponds to 2MASS 07495348+0430238. The steps are 2' in RA and 11' in Dec; north is up, and east to the left. For the extreme positions, the spectra scaled by a factor 10 are also shown in dashed lines.

& Gérard, 2004). In the direction of the DDK cloud, we encounter no effective confusion by Galactic H $_{\rm I}$ at $V_{\rm lsr} > 30~{\rm km~s^{-1}}$, in agreement with the inspection of the LAB Survey of Galactic H $_{\rm I}$ (Kalberla et al. 2005). We find no difference between the position-switch spectra at $\pm\,8'$ and at $\pm\,12'$, so that we can set an upper limit of 12' for the DDK cloud extension in RA. It is noteworthy that these two position-switch spectra perfectly agree with the baseline-subtracted frequency-switch spectrum obtained with the telescope pointing directly on the 2MASS star (cf. Fig. 1, with a conversion factor, 2.15 K/Jy).

We have also obtained data in the position-switch mode at +11' (north) and -11' (south) with off-positions at $\pm 2'$, $\pm 4'$, and $\pm 12'$ (east-west), and at +22' (north) and -22' (south), with off-positions at $\pm 12'$ (east-west). All these data are used to construct the H I map that is presented in Fig. 2. By integrating the individual spectra over the map, we obtain the integral spectrum of the DDK cloud that is presented in Fig. 3.

This spectrum shows a Gaussian-like profile of width, FWHM = $2.73 \, \mathrm{km \, s^{-1}}$, and centered at V_{lsr} = $47.74 \, \mathrm{km \, s^{-1}}$ (Table 1, "Total"). The H_I line profile is narrow and can be used to set an upper limit on the average hydrogen kinetic temperature of $\sim 170 \, \mathrm{K}$. Emission in excess of the Gaussian profile may be present from 42 to 53 km s⁻¹ at

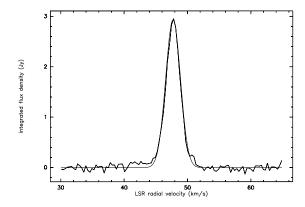


Fig. 3. Integrated H I spectrum of the DDK cloud obtained with the NRT. A fit with one Gaussian ($V_c = 47.74 \text{ km s}^{-1}$, FWHM = 2.73 km s⁻¹) is represented by a thin line. An excess of emission can be seen in the wings of the profile.

Table 1. H_I line profile parameters obtained with the NRT data. In parentheses, we give formal errors resulting from the H_I-line Gaussian-fits (Landman et al. 1982).

-	V_{c}	FWHM	Intensity	Integrated flux
	$(km s^{-1})$	$(km s^{-1})$	(Jy)	$(Jy\times km s^{-1})$
4′ W	47.96 (0.02)	2.56 (0.03)	0.59 (0.01)	1.62 (0.05)
2′ W	47.80 (0.01)	2.61 (0.01)	1.65 (0.01)	4.58(0.05)
"on"	47.64 (0.01)	2.72 (0.01)	2.02 (0.01)	5.84 (0.01)
2' E	47.58 (0.01)	2.91 (0.02)	1.24(0.01)	3.85 (0.05)
4′ E	47.70 (0.04)	2.94 (0.06)	0.39(0.02)	1.23 (0.05)
22′ N	47.89 (0.10)	2.44 (0.10)	0.15 (0.01)	0.38 (0.05)
11′ N	47.83 (0.01)	2.82 (0.01)	1.24(0.01)	3.72(0.02)
11′ S	47.48 (0.01)	2.75 (0.01)	1.06(0.01)	3.12 (0.02)
22′ S	47.16 (0.10)	3.45 (0.15)	0.15 (0.01)	0.56(0.05)
Total	47.74 (0.01)	2.73 (0.02)	2.95 (0.03)	8.59 (0.11)

a level of $\sim 20\,\text{mJy}$. The integrated area is $8.6\,\text{Jy}\times\text{km\,s}^{-1}$, which translates to a hydrogen mass for the enigmatic cloud, at a distance d expressed in kpc, $M_{HI}=2.03\times d^2\,M_\odot$. The line profiles at the other positions in the map are also Gaussian-like, the intensity being slightly larger west than east. The center of mass of the H $_{\rm I}$ emission thus appears offset by $-0.3\pm0.1'$ (west) with respect to the 2MASS star. The source is slightly resolved in RA, with a size of $4.3\pm0.3'$ (FWHM). There is also a possible offset in Dec., $+1.1\pm0.3'$ (north), and an extension that we estimate at $\sim 9\pm3'$. Finally the centroid velocity is redshifted north and west, and blueshifted south and east as compared to the center (see Table 1), in agreement with the velocity gradient reported by DDK2008.

In general, our results agree with those of DDK2008. We confirm that the source is isolated and compact, and that it shows an ordered velocity gradient. However, we find a narrower profile (FWHM = $2.73\,\mathrm{km\,s^{-1}}$, Table 1), than theirs $(3.4\pm0.18\,\mathrm{km\,s^{-1}})$. Our estimate is also consistent with that obtained independently on the baseline subtracted frequency-switch spectrum presented in Fig. 1 (FWHM = $2.91\pm0.1\,\mathrm{km\,s^{-1}}$).

2.2. CO observations

The DDK H_I cloud was observed in CO (1-0) and (2-1) with the IRAM-30m telescope on Dec. 5, 2008. We selected three posi-

Table 2. Positions observed in CO with the IRAM 30-m telescope.

	α (2000.0)	δ (2000.0)	111	b ^{II}
H i peak: A1	07 49 54	04 32 30	215.555	15.068
A2	07 49 50	04 32 20	215.550	15.052
A3	07 49 54	04 29 00	215.609	15.042

tions, centered on peaks of H_I emission visible on the VLA map (Table 2), because in the Helix Nebula H_I emission was found in the outer parts where CO is also present (Rodríguez et al. 2002, Young et al. 1999). The telescope beamwidths (FWHM) are 21" at 115 GHz and 11" at 230 GHz, and are thus smaller than the VLA synthesized beam (45"×35"). The data were obtained with the VESPA autocorrelator at different spectral resolutions and bandwidths (resolution 10 kHz and 20 kHz, bandwidths 35 MHz and 53 MHz, respectively at 3 mm and resolution 20 kHz and 40 kHz with bandwidths of 35 MHz and 107 MHz, respectively, at 1 mm) and, simultaneously, with a low resolution filter bank (resolution 1 MHz, bandwidth 256 MHz). The system temperature was 450 K at 3 mm, and 700 K at 1 mm. We obtained spectra with an rms noise of 0.016 K (T_{mb}) at 115 GHz, for a resolution of 2.6 km s⁻¹, and of 0.063 K at 230 GHz, for a resolution of 1.3 km s⁻¹. No emission was detected in any of the three positions.

We follow the Jura et al. (1997) approach for estimating upper limits on the CO column densities in the three lines-of-sight. We assume that CO is optically thin and warm ($\gg 11$ K), and use their equation (4):

$$N(CO) = 4.32 \ 10^{13} \ T_{ex} \ \int T_{mb} \ dV$$
, for CO(1-0), and $N(CO) = 1.08 \ 10^{13} \ T_{ex} \ \int T_{mb} \ dV$, for CO(2-1),

with N(CO) in cm $^{-2}$ and V in km s $^{-1}$. For T_{ex} , we adopt, as an upper limit, the upper limit on the H $_{\rm I}$ kinetic temperature that was obtained in the previous section ($T_{\rm K}=170~{\rm K}$). By integrating our CO spectra over the range $42–53~{\rm km\,s^{-1}}$, the maximum velocity range over which we found H $_{\rm I}$ emission (cf. Sect. 2.1), we can thus derive conservative upper-limits of $6~10^{14}~{\rm cm^{-2}}$ and $4~10^{14}~{\rm cm^{-2}}$, respectively from the two lines, on the column density in CO. This may be compared to the peak CO column density of $\sim 1.5~10^{16}~{\rm cm^{-2}}$ obtained by Young et al. (1999) at an angular resolution of 31" in the Helix Nebula, for a corresponding peak H $_{\rm I}$ density of $1.2~10^{20}~{\rm cm^{-2}}$ (Rodríguez et al. 2002).

3. Discussion

The DDK H I cloud has no counterpart at other wavelengths. It is not seen on the IRAS maps and it has not been detected at 870 μ m with the Large Bolometer Camera on the 12-m APEX antenna (DDK2008), showing no detection of cold dust, and no evidence of heating by an internal source. There is no obvious counterpart on the NRAO VLA Sky Survey (NVSS; Condon et al. 1998) continuum map obtained at 1.4 GHz.

However, a 2MASS star was pointed out by DDK2008 at about the center of the cloud. The cross-identification with the USNO-B1.0 and Tycho-2 catalogs shows this star has an apparent proper motion of +4 mas/yr in RA and +30 mas/yr in Dec (PA = -8°). The distance is not known. Its near-infrared colors (Table 3) correspond to that of an F-type star, but the optical data correspond rather to an A-type star. It has no mid or far-infrared counterpart, but has been detected in the ultraviolet by GALEX.

There are also several faint stars around the DDK cloud. Interestingly among them there is a high proper-motion one at about 8' south moving away from the H_I cloud (NLTT 18499,

Table 3. Photometry of 2MASS 07495348+0430238 and NLTT 18499, without correction, and with a correction corresponding to A_v = 0.26 (R=3.1; IR/Visual: Fitzpatrick 1999, UV: Rey et al. 2007). Sources: IR (2MASS), Visual (Tycho-2, USNO-B1.0, Droedge et al. 2006), UV (GALEX, AB system).

	2MASS		NLTT	
	$A_v = 0$	$A_v = 0.26$	$A_v = 0$	$A_v = 0.26$
K _s	10.22	10.19	13.58	13.55
Н	10.24	10.19	13.74	13.69
J	10.50	10.43	14.24	14.07
I	10.94	10.81	15.1	15.0
R	11.6	11.4	16.0	15.8
V	11.6	11.4	_	_
В	11.7	11.4	17.3	17.0
NUV	15.57	14.82	_	_
FUV	21.4	20.7	_	_

+56 mas/yr in RA and -190 mas/yr in Dec, Lepine & Shara 2005).

3.1. The circumstellar-shell hypothesis

Following DDK2008, we adopt arbitrarily a distance of 400 pc, which translates to a height above the Galactic Plane of 100 pc $(b^{II} = +15^{\circ})$. The DDK cloud mass in atomic hydrogen would therefore be 0.32 M_{\odot} , and the size, 0.6 pc. These estimates are typical of circumstellar shells around evolved red giants, carbon stars or Planetary Nebulae (Gérard & Le Bertre 2006). In this context, as the H_I mass scales as d^2 , the DDK cloud cannot be much further than 1 kpc. The narrow and Gaussian-like line profile is also typical of those obtained for such sources. Libert et al. (2007) have developed a model in which such a line profile results from the slowing-down of a stellar wind by ambient matter. In this model a "detached shell" is built over time, with an inner radius where the stellar outflow is abruptly slowed-down (termination shock) and an outer radius where external matter is compressed by the expanding shell (bow shock). The detached shell is thus formed of compressed circumstellar and interstellar materials, which are heated when crossing the shocks, and cooling-down after that. They applied this model to the detached shell observed around the carbon star Y CVn (Izumiura et al. 1996), and were able to reproduce satisfactorily the H_I line profiles obtained at different positions.

In order to check the applicability of this model to the DDK cloud, we have performed a calculation with the parameters given in Table 4. We take a star undergoing mass loss, at a rate of 3 10⁻⁷ M_☉ yr⁻¹ (in atomic hydrogen) and with an expansion velocity, $V_{exp} = 6 \text{ km s}^{-1}$, for $\sim 10^6 \text{ years}$. The expansion velocity has been selected such as to cover the range of H_I emission, from 42 to 53 km s⁻¹. In Fig. 4, the results (solid lines) are compared to observations. As the model is spherical, we have averaged the east and west spectra. The H_I line profiles and intensities are reproduced satisfactorily. In Fig. 5, we present the H_I column density derived from the model; it gives a peak N_{H} ~ 1.8 10^{20} cm⁻² at 2.1' in accordance with the VLA results (DDK2008). However, in contrast to the Y CVn detached shell, there is no evidence of a red giant associated to the DDK H_I cloud (see below). Therefore the model that is presented here only demonstrates that the observed properties of the enigmatic cloud, and in particular its peculiar H_I line profile, can be easily accounted for by mass loss from a stellar source.

The H_I image of the DDK cloud obtained with the VLA by DDK2008 shows some similarities to that observed by

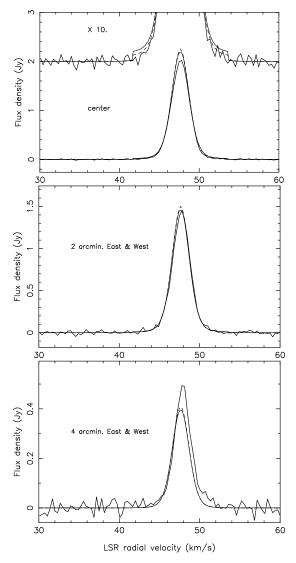


Fig. 4. Comparison between the H_I line profiles obtained with the NRT (thick lines) and the model of a detached shell around an AGB star discussed in Sect. 3.1 (thin and dashed lines). Top: central spectrum; middle: average of the two spectra at +2' (east) and -2' (west); bottom: average of the two spectra at +4' and -4'.

Table 4. Model parameters (d = 400 pc). The notations are the same as in Libert et al. (2007).

M (in hydrogen)	$3 \ 10^{-7} \ \mathrm{M}_{\odot} \mathrm{yr}^{-1}$
μ	1.3
t_1	5.7 10 ⁴ years
t_{DS}	9.7 10 ⁵ years
r_1	0.17 pc (1.5')
\mathbf{r}_f	0.29 pc (2.53')
r_2	0.35 pc (3')
$T_0(\equiv T_1^-), T_1^+$	20 K, 1070 K
$T_f (= T_2)$	92 K
$v_0 (\equiv v_1^-), v_1^+$	$6 \text{ km s}^{-1}, 1.5 \text{ km s}^{-1}$
\mathbf{v}_f	$0.04 \; \mathrm{km} \; \mathrm{s}^{-1}$
\mathbf{v}_2	$0.6 \mathrm{km} \mathrm{s}^{-1}$
n_1^-, n_1^+	$5.2 \mathrm{H}\mathrm{cm}^{-3}, 21.0 \mathrm{H}\mathrm{cm}^{-3}$
$\mathbf{n}_f^-, \mathbf{n}_f^+$	$301.0 \mathrm{Hcm^{-3}}$, $2.2 \mathrm{Hcm^{-3}}$
n_2	$1.6 \mathrm{Hcm^{-3}}$
$M_{r < r_1}$ (in hydrogen)	$1.7 \ 10^{-2} \ \mathrm{M}_{\odot}$
$M_{DT,CS}$ (in hydrogen)	0.29 M _☉
$M_{DT,EX}$ (in hydrogen)	$3.3 \ 10^{-3} \ \mathrm{M}_{\odot}$

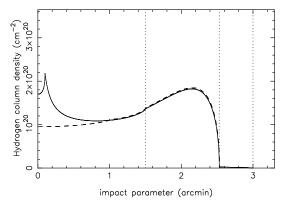


Fig. 5. Atomic hydrogen column density profile for the detached shell model discussed in Sect. 3.1. The vertical dotted lines mark the radii r_1 , r_f and r_2 of the model (see Table 4).

Rodríguez et al. (2002) in the Helix Nebula (NGC 7293), a Planetary Nebula (PN) and therefore a source in a late stage of evolution after the Asymptotic Giant Branch (AGB). Their data obtained with the VLA in the DnC configuration reveal a ring of atomic hydrogen, with the H $_{\rm I}$ emission concentrated in clumps. This H $_{\rm I}$ ring has a diameter of 12′, or 0.7 pc at a distance of 200 pc. The emission coincides with the continuum emission at 1.4 GHz and seems to delineate the outer parts of the ionized gas. Gérard & Le Bertre (2006) estimate the total atomic hydrogen mass in the Helix Nebula at 0.26 M_{\odot} . CO emission has also been detected around the ionized gas (Young et al. 1999). It delineates the same ring as in H $_{\rm I}$, but is also found in small cometary globules embedded in the ionized gas (Huggins et al. 2002).

On the other hand, there are important differences between the Helix Nebula and the DDK cloud. The Helix Nebula exhibits a much broader global line profile in H_I (FWHM $\sim 35 \text{ km s}^{-1}$, Gérard & Le Bertre 2006). Molecular gas (CO, Sect. 2.2) has not been detected in the DDK cloud at the three peaks of H_I column density that have been observed, which weakens our working hypothesis unless CO is concentrated in small globules that we have missed. The Helix Nebula, like many other PNs, has been detected in continuum emission at 1.4 GHz in the NVSS, whereas no such emission is detected for the DDK cloud. IRAS and ISO observations of the Helix Nebula at 90 and 160 μm show extended (~ 20') thermal emission by dust with a possible contribution of emission lines (Speck et al. 2002). There is no evidence for thermal emission by dust in the DDK cloud (DDK2008). The Helix Nebula is a well-known emission-line source (PK 036-57), but there is no emission-line source associated with the DDK cloud. Also an inspection of the Southern H α Sky Survey Atlas (Gaustad et al. 2001) shows no emission close to its position. Thus there is presently no evidence for ionized material in the DDK cloud, and it seems difficult to associate it with a PN.

DDK2008 suggest that the H I cloud could be formed by mass loss from the star detected in the 2MASS survey. The colors of this star are not compatible with those of red giants. At a distance of 400 pc, its luminosity should be on the order of $3\pm1~L_{\odot}$ (depending on its exact energy distribution), much too low for being a star in transition between the AGB and the PN stages. In fact from the non-detections at IRAS wavelengths and at 870 μ m, there is no evidence of a luminous star inside the DDK cloud.

In the context of the circumstellar-shell hypothesis, there is only one option left: that the DDK cloud is a fossil circum-

stellar shell of a source that is now in a post-PN phase. This source would then be evolving towards the white dwarf stage, i.e. it would be a stellar core of decreasing luminosity and temperature such that there is no significant heating nor ionization close to the DDK cloud. An obvious candidate would be 2MASS 07495348+0430238. However this object seems peculiar: the optical and near-infrared colors do not match well. It could be a variable star, a star with an infrared excess, or a binary system. Also, the stellar remnant might have moved away from its circumstellar shell (e.g. Smith 1976), and nearby stars, such as NLTT 18499, should also be considered. Radial velocity measurements could help to select the best candidate. A parallax would constrain the distance, and, *in this context*, the physical characteristics of the DDK cloud.

Due to the large scale of the circumstellar shell, a cessation of the mass loss by the central star would not affect strongly the H I emission before several 10^4 years (i.e. before a lapse smaller than the time needed by stellar matter to reach the termination shock in r_1 , 5.7 10^4 years). In order to illustrate this effect, we have made a second run of our model, with only t_1 reduced from 5.7 10^4 years to 2 10^4 years, all other input parameters being kept equal. Only the central part $(r < r_1)$ is affected by this modification because the wind is supersonic up to the termination shock. The results are shown in dashed lines in Figs. 4 and 5. The predicted H I-profiles are almost indistinguishable, except in the wings of the central-position line profile.

We should also account for the lack of H α and CO emission. For an average density of 10 cm⁻³, the recombination time of electrons is $\sim 10^4$ years, which sets a lower limit on the time since the hypothetical source of ionization should have been switched-off. The timescale for CO photo-dissociation in the ISM is ~ 200 years (Mamon et al. 1988). However, CO is self-shielded and may survive for a much longer time, up to 10⁵ years, depending on the mass-loss rate and expansion velocity, and possibly more if the medium is inhomogeneous. The timescale for the dispersion of circumstellar shells around evolved stars is also uncertain. It probably depends on the wind history, on the properties of the ambient ISM and on the velocity of the central star relative to this medium (Villaver et al. 2002, 2003). H_I observations show that these structures may have a lifetime of at least several 10⁵ years (Gérard & Le Bertre 2006, Libert et al. 2007). Some post-PN circumstellar shells, old enough to escape detection in $H\alpha$ and CO, should then be expected. However, up to now none has been identified. The DDK cloud would then be the first specimen, and we probably need to identify other cases before reaching a firm conclusion on the circumstellar-shell hypothesis.

3.2. The IVC/HVC hypothesis

The DDK cloud could also be associated with the population of high galactic latitude clouds that are found at high velocity, $|V_{\rm lsr}| > 70~{\rm km\,s^{-1}}$ (High-Velocity Clouds, HVC), or at lower velocity (Intermediate-Velocity Clouds, IVC). In particular de Heij et al. (2002a) have identified a population of small ($\leq 1^{\circ}$ FWHM) and isolated high-velocity clouds (compact HVC, or CHVC) sharply bounded in angular extent. A follow-up study with the Westerbork Synthesis Radio Telescope shows a corehalo morphology similar to that seen in the DDK H I cloud (de Heij et al. 2002b, see e.g. CHVC 120-20-443 in their figure 2). The enigmatic cloud has a radial velocity lower than the characteristic velocity of HVC, but we have no information on its transverse velocity. Perhaps more confounding, the velocity dispersion in CHVC (typically 20 km s^-1) is much larger than that

in the DDK cloud. IVC have probably a two-phase structure with bright clumps and a diffuse envelope similar to that of HVC (Smoker et al. 2002, Haud 2008).

Absorption H I-line surveys made with Arecibo and the Giant Metrewave Radio Telescope (Heiles & Troland 2003, Mohan et al. 2004) have revealed the presence in the ISM of many small clouds, at low and intermediate radial velocity, with hydrogen at a temperature in the range 50-200 K, comparable to that in the DDK cloud. These clouds might be associated to the population of discrete H I clouds discovered in emission with the Green Bank Telescope by Lockman (2002). The latter seem to follow Galactic rotation, to have a peak $N_{\rm H}$ of a few times $10^{19}~{\rm cm}^{-2}$, and linewidths in the range of a few to tens of km s $^{-1}$. Lockman (2002) proposes that they are located in the Galactic halo, and have sizes of few tens of parsecs and typical masses of 50 M_{\odot} . We cannot exclude that the DDK cloud would be a member of this population, on the low side of its velocity-dispersion distribution.

The origin of CHVC/IVC is a matter of debate, the most critical difficulty being their uncertain distance. In fact as, up to now, post-PN circumstellar shells have still not been identified, we would like to raise the possibility that some of these objects may hide among the population of CHVC/IVC. Désert et al. (1990) have already noted a coincidence between an IVC, which they detected in CO, and a white dwarf. It is also known that some evolved stars at high-galactic latitude are associated with extended gaseous tails that show a cometary morphology in H1 evocative of IVC/HVC (Matthews et al. 2008, Libert et al. 2008).

3.3. The extragalactic hypothesis

DDK2008 raised the possibility that the H_I cloud they discovered might be extragalactic in origin. In this case, the requirement that the cloud be gravitationally bound imposes an upper limit on its distance of ~530 kpc (in order that its H_I mass does not exceed its virial mass). Placed at a nearer distance, the H_I mass alone would no longer be able to account for the observed linewidth, implying that some additional "dark" component must be present. DDK2008 therefore suggested that the cloud might be an example of a "dark galaxy"—a galactic system too low in mass to have become unstable to star formation. This hypothesis is of particular interest, since the existence of large numbers of low-mass satellites to the Milky Way (the smallest of which are not expected to have formed stars) has been predicted by cold dark matter models of galaxy formation (e.g., Klypin et al. 1999; Moore et al. 1999).

Recently Ryan-Weber et al. (2008) discovered an unusual dwarf galaxy, Leo T, whose H_I properties share some interesting similarities with the DDK cloud. Both Leo T and the DDK cloud have similar angular sizes (~ 5') and clumpy, ellipticalshaped H_I morphologies. Placed at the adopted distance of Leo T (420 kpc), the DDK cloud and the Leo T dwarf would also have comparable H I masses $(3.4 \times 10^5 M_{\odot})$ and $2.8 \times 10^5 M_{\odot}$, respectively). However, there are several noteworthy differences between these two objects. The Leo T dwarf has a larger H I velocity width (\sim 7 km s⁻¹), and its velocity field shows no signatures of rotation. Indeed, lack of ordered rotation tends to be a generic feature of the lowest mass dwarf galaxies (e.g., Grebel 2008). Another key difference is that Leo T has a ratio of dynamical mass to H_I mass ~50 (and very few stars), implying a large dark matter fraction. In contrast, $M_{\rm dyn}/M_{\rm HI} \sim 2$ for the DDK cloud if located at the same distance. After accounting for the mass contribution of helium, this leaves little room for a significant amount of "dark" material.

If the DDK cloud is truly a rotating disk, then its measured rotational velocity should be corrected for the disk's inclination to our line-of-sight. Assuming the disk is circular with an intrinsic flattening $q \sim 0.1$, its measured H I axial ratio (b/a=0.7; DDK2008) implies $i \approx 46^{\circ}$, based on the standard relation

$$\cos^2 i = \frac{\left(\frac{b}{a}\right)^2 - q_0^2}{1 - q_0^2}$$

Thus the true peak rotational velocity is $V_{\rm rot}/\sin i \approx 1.4 \ {\rm km \, s^{-1}}$. Yet, this value is still extraordinarily small, leading to a difficulty in explaining how such a low-mass system could have retained an observable quantity of cold, neutral gas to the present day.

Current galaxy formation models predict that the reionization of the intergalactic medium at high redshift will suppress gas accretion onto galactic potentials with circular velocities $V_{\rm circ} \lesssim 20\text{-}30~{\rm km\,s^{-1}}$ (e.g., Bullock et al. 2000). Even if such low-mass structures were able to collapse, their gas would be expected to rapidly photoevaporate (Barkana & Loeb 1999). Furthermore, gas would be prevented from condensing back onto such structures during later epochs, since the characteristic mass scales for structure formation in the intergalactic medium exceed the mass of these "mini-halos" (e.g., Gnedin 2000).

Ricotti (2009) proposed that this latter problem could be partly overcome by the increasing central concentration of the galaxy potentials and the decreasing temperature of the intergalactic medium as a function of decreasing redshift. However, his models predict that the lowest mass galaxies able to cool below 10^4 K within a Hubble time have $V_{\rm circ} \sim 5-7$ km s⁻¹—several times higher than the DDK cloud. Moreover, the dynamical masses of the smallest galaxies are predicted to exceed their gas masses by more than an order of magnitude. The latter discrepancy could be alleviated by placing the DDK cloud at a smaller distance (e.g., comparable to the Magellanic Clouds). However, in this case, any accreted gas would likely be depleted via ram pressure stripping during passage through the Galactic corona (Mayer et al. 2006).

Finally, there may be some difficulty accounting for the presence of an H I column density minimum or "hole" near the center of rotation of the DDK cloud in an extragalactic scenario. While such features are common in dwarf galaxies, their origins are most likely tied either directly or indirectly with star formation, arising from energy injection from stellar winds and/or supernovae (e.g., Kerp et al. 2002), or from a combination of turbulence and thermal and gravitational instabilities (Dib & Burkert 2005). In summary, while an extragalactic origin for the DDK cloud cannot yet be strictly excluded, it appears unlikely in light of the available data for the cloud and our present theoretical understanding of the formation and evolution of the lowest mass galaxies.

4. Conclusions

The H I emission from the DDK cloud is well separated from the rest of the Galactic emission. It shows a narrow line profile that can be fitted with one Gaussian of width $2.8\,\mathrm{km\,s^{-1}}$ and that is centered at $V_{lsr} = 47.7\,\mathrm{km\,s^{-1}}$. The cloud has a size of 4′ in RA, and for a distance d expressed in kpc, a mass in atomic hydrogen of $2\times d^2\,\mathrm{M}_\odot$. The rotational lines of CO (2-1 and 1-0) have not been detected.

The H_I line profiles are compatible with the model of a detached shell around an AGB star, which we have developed for the carbon star Y CVn. However, owing to the absence of a luminous and/or hot central star, we discard the possibility that the

DDK cloud is related to a mass-losing red giant, a post-AGB object or a planetary nebula central star. In the context of the circumstellar shell hypothesis, we suggest that the DDK cloud could be a fossil shell left over by a stellar core (still to be identified, but possibly associated with the 2MASS star pointed out by DDK2008) that is now evolving towards the white-dwarf stage.

With a core-halo morphology, the DDK H_I cloud might also be related to a compact HVC/IVC, although the narrow H_I linewidth would be atypical. An extragalactic origin can also be considered, but again appears improbable in view of the small velocity dispersion.

Presently the circumstellar shell hypothesis is the only one that can easily account for the small linewidth. If this hypothesis proves to be correct, the DDK cloud might offer the first occasion to study a post-PN stellar remnant together with its fossil shell.

Acknowledgements. The Nançay Radio Observatory is the Unité scientifique de Nançay of the Observatoire de Paris, associated as Unité de Service et de Recherche (USR) No. B704 to the French Centre National de la Recherche Scientifique (CNRS). The Nançay Observatory also gratefully acknowledges the financial support of the Conseil Régional de la Région Centre in France. IRAM is supported by INSU/CNRS (France), MPG (Germany), and IGN (Spain). This research has made use of the SIMBAD and VizieR databases, operated at CDS, Strasbourg, France and of the NASA's Astrophysics Data System.

References

Barkana, R. & Loeb, A. 1999, ApJ, 523, 54 Bullock, J.S., Kravtsov, A.V., & Weinberg, D.H. 2000, ApJ, 539, 517 Condon, J.J., Cotton, W.D., Greisen, E.W., et al. 1998, AJ, 115, 1693 Dedes, L., Dedes, C., & Kalberla, P.W.M. 2008, A&A, 491, L45 (DDK2008) Désert, F.-X., Bazell, D., & Blitz, L. 1990, ApJ, 355, L51 Dib, S. & Burkert, A. 2005, ApJ, 630, 238 Droege, T.F., Richmond, M.W., Sallman, M.P., & Creager, R.P. 2006, PASP, 118, Fitzpatrick, E.L. 1999, PASP, 111, 63 Gaustad, J.E., McCullough, P.R., Rosing, W., & Van Buren, D. 2001, PASP, 113, 1326 Gérard, E. & Le Bertre, T. 2006, AJ, 132, 2566 Gnedin, N.Y. 2000, ApJ, 542, 535 Grebel, E. 2008, in Dark Galaxies and Lost Baryons, Proceedings IAU Symposium No. 244, J. I. Davies & M. J. Disney (eds.), 300 Haud, U. 2008, A&A, 483, 461 de Heij, V., Braun, R., & Burton, W.B. 2002a, A&A, 391, 159 de Heij, V., Braun, R., & Burton, W.B. 2002b, A&A, 391, 67 Heiles, C. & Troland, T.H. 2003, ApJ, 586, 106 Huggins, P.J., Forveille, T., Bachiller, R., et al. 2002, ApJ, 573, L55 Izumiura, H., Hashimoto, O., Kawara, K., Yamamura, I., & Waters, L.B.F.M. 1996, A&A, 315, L221 Jura, M., Kahane, C., Fischer, D., & Grady, C. 1997, ApJ, 485, 341 Kalberla, P.M.W., Burton, W.B., Hartmann, D., et al. 2005, A&A, 440, 775 Kerp, J., Walter, F., & Brinks, E. 2002, ApJ, 571, 809 Klypin, A., Kravtsov, A.V., Valenzulela, O., & Prada, F. 1999, ApJ, 522, 82 Landman, D. A., Roussel-Dupré, R., & Tanigawa, G. 1982, ApJ, 261, 732 Le Bertre, T. & Gérard, E. 2004, A&A, 419, 549 Lepine, S. & Shara, M.M. 2005, AJ, 129, 1483 Libert, Y., Gérard, E., & Le Bertre, T. 2007, MNRAS, 380, 1161

684, 603
Matthews, L.D. & Reid, M.J. 2007, AJ, 133, 2291
Mayer, L., Mastropietro, C., Wadsley, J., Stadel, J., & Moore, B. 2006, MNRAS, 369, 1021
Mohan, R., Dwarakanath, K. S., & Srinivasan, G. 2004, JAA, 25, 185
Moore, B., Ghigna, S., Governato, G., et al. 1999, ApJ, 524, L19
de Pater, I., Palmer, P., & Snyder, L.E. 1991, Ap&SS Library, 167, 175
Rey, S.-C., Rich, R. M., Sohn, S.T., et al. 2007, ApJS, 173, 643
Ricotti, M. 2009, MNRAS, 392, L45
Rodríguez, L.F., Goss, W.M., & Williams, R. 2002, ApJ, 574, 179
Ryan-Weber, E.V., Begum, A., Oosterloo, T., et al. 2008, MNRAS, 384, 535
Smith, H. 1976, MNRAS, 175, 419

Libert, Y., Le Bertre, T., Gérard, E., & Winters, J.M. 2008, A&A, 491, 789

Matthews, L.D., Libert, Y., Gérard, E., Le Bertre, T., & Reid, M.J. 2008, ApJ,

Mamon, G.A., Glassgold, A.E., & Huggins, P.J. 1988, ApJ, 328, 797

Lockman, F.J. 2002 ApJ, 580, L47

Smoker, J.V., Haffner, L.M., Keenan, F.P., Davies, R.D., & Pollacco, D. 2002, MNRAS, 337, 385

Speck, A. K., Meixner, M., Fong, D., et al. 2002, AJ, 123, 346

Villaver, E., García-Segura, G., & Manchado, A. 2002, ApJ, 571, 880 Villaver, E., García-Segura, G., & Manchado, A. 2003, ApJ, 585, L49 Young, K., Cox, P., Huggins, P.J., Forveille, T., & Bachiller, R. 1999, ApJ, 522, 387